2D-modelling of pellet injection in the poloidal plane : results of numerical tests

Paraskevas Lalousis

2D-Modelling of pellet injection in the poloidal plane: results of numerical tests

P. Lalousis *
Institute of Electronic Structure and Laser, Foundation for Research and Technology, Association Euratom - Hellenic Republic, Heraklion 71110,Greece.

A time-dependent two-dimensional resistive MHD code is being developed for computing the expansion of pellet-produced clouds in the poloidal plane. The expansion of the ablated substance in the third (toroidal) direction and its mixing with the background plasma is also taken into account.
The various components of the code complex are being tested by means of simplified model calculations. In the present paper, results pertaining to the expansion and drift of a high-density plasmoid in a magnetically confined homogeneous background plasma are reported. The confining (toroidal) field may be uniform or has a prescribed gradient. In this test phase, the 2D code is ran in a one-dimensional mode: it is assumed that all changes are restricted to the 'x' direction, which represents in our case the radial direction in the poloidal plane (the domain is assumed to extend to infinity in the vertical 'y' direction).
In the present check runs, a high-density fully ionized plasmoid of finite extent (initial width $l_0 = 4$cm, $n_{p0} = 10^{23} m^{-3}$, $T_{p0} = 20$ eV) is placed in the middle of a homogeneous background plasma with $n_0 = 10^{20} m^{-3}$ and $T_0 = 1$ keV. The size (total width) of the computational domain is 100 cm. At time = 0, the plasmoid is set free and its expansion dynamics is followed-up numerically. Because of the lack of reliable physical boundary conditions at the left and right boundaries of the computational domain, (flux continuity and/or zero gradients are assumed in the present computations) results obtained after the disturbance has reached the boundaries are irrelevant.
The full set of time-dependent resisitve MHD equations [1] consisting of the conservation equations for mass, momentum, and energy, and supplemented by Maxwell's equations, a number of rate equations (ionization rate, etc.), and equations describing diffusive transport processes (internal energy, magnetic field) is solved by applying a 2nd order Godunov numerical scheme and the GMRES method. The numerical scheme is based on a Riemann solver with Roe's approximation.
In this analysis, three cases are considered in detail: a) The magnetic field strength is zero; b) An initially homogeneous magnetic field of B = 2 Tesla is applied over the whole domain; c) A spatially varying magnetic field with a gradient of the order of 1 tesla/m is applied over the width of the plasmoid.
a) Considering the first scenario corresponding to zero magnetic field, the plasmoid expansion is symmetric with respect to the plasmoid axis.
Figure 1a shows the velociy distribution along the x-axis for three time instants (0.5, 1.0, and 5.0 μ). The curve corresponding to 5 μs may be disregarded: prior to this time instant the disturbance has already reached the boundary of the computational domain.

The spatial and time variation of the temperature, density, and pressure distributions are given in Figs. 1b, 1c, and 1d, respectively. The development of a hydrodynamic shock in the initially undisturbed background plasma is apparent. The temperature distribution (Fig.1b) too indicates the presence of a shocked regions with a local elevation of about 12% of the background temperature. In the core region, the temperature remains of the order of 20 eV (initial value). The heat capacity of the high-density core is much too high to obtain notable temperature changes on the time scale considered.
The pressure ratio associated with the quasi-steady expansion phase (see the first two curves) is related to the respective temperature ratio characterizing the shock wave by the classical Rankine-Hugoniot relations. In our case, the computed value compares well with the calculated analytical value (1.126).
b) If a homogeneous magnetic field of B = 2 Tesla is applied over the whole domain, the $v \times B$-induced ring currents decelerate and practically stop the plasmoid expansion within a few μs (ignoring particle diffusion).
Figure 2a and 2b show the particle density and magnetic field distributions for three time instants: 1.0, 2.5 and 5.0 μs, respectively. The expansion is still symmetric with respect to the midplane. As can be seen, the confinement length ('radius') is, for the case considered, about 5 cm.
A magnetic cavity forms inside the plasmoid, the maximum decrease of the magnetic field strength being about 25 % in the centre. The curves indicate that the radial confinement of the plasmoid is associated with a number of (damped) oscillations, in ageement with the results of earlier magnetospheric barium plasma and pellet cloud simulations [2].
c) Applying a magnetic field gradient ower the initial width of the spatially limited plasmoid, the time development of the distributions becomes asymmetric: the disturbances become shifted, i.e. they propagate, in the direction of the decreasing magnetic field strength. In the given case, the initial (input) magnetic field strength decreases from 2.01 Tesla at the l.h.s. boundary of the plasmoid to 1.99 Tesla at the r.h.s. boundary (0.5 Tesla/m gradient).
Figures 3a and 3b show the resulting density and temperature distributions for three time instants. The shift of the plasmiod to the low-field side is apparent.
As before, the background plasma is being shock-heated, the maximum temperature elevation in the shocked region being about 15 % The average drift velocity deducible from this plot for the first 4 to 5 μs of the plasmoid motion is about 5×10^3 m/s.

Acknowledgement

* This is collaborative work with Max-Planck Institut für Plasmaphysic Garching/Greifswald, the collaboration with Drs L.L.Lengyel and R.Schneider is very much appreciated.

References

[1] P.J. Lalousis and L.L. Lengyel, Nucl. Fusion Vol. 40 (2000), p. 1511.
[2] L.L. Lengyel Phys. Fluids Vol. 31 (1988), p. 1577.

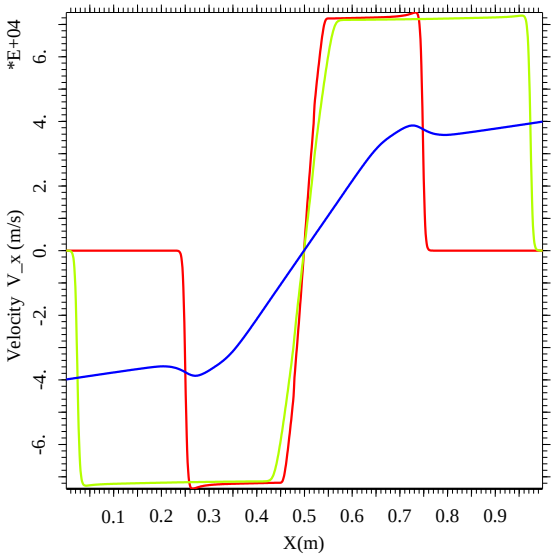

Figure 1.a Velocity profile, at $0.5\mu s$(red), $1\mu s$ (green) and at $5\mu s$ (blue).

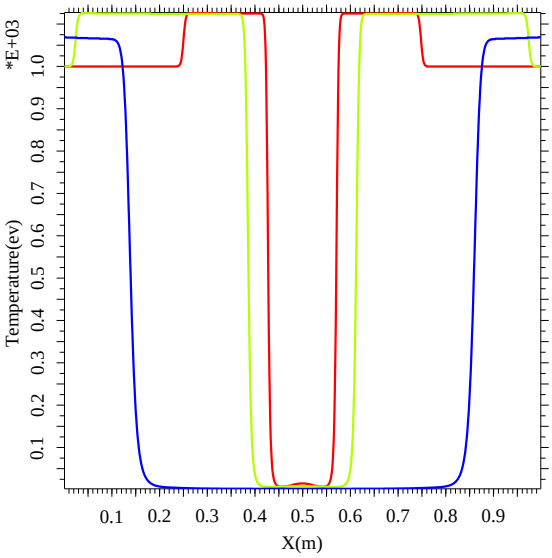

Figure 1.b Temperature profile, at $0.5\mu s$(red), $1\mu s$ (green) and at $5\mu s$ (blue).

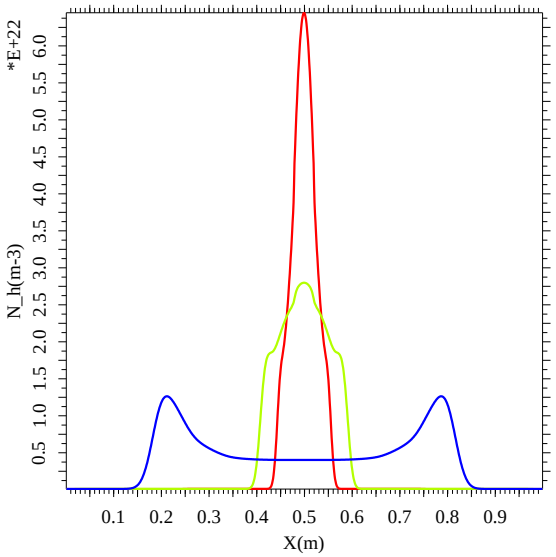

Figure 1.c Particle density profile, at $0.5\mu s$(red), $1\mu s$ (green) and at $5\mu s$ (blue).

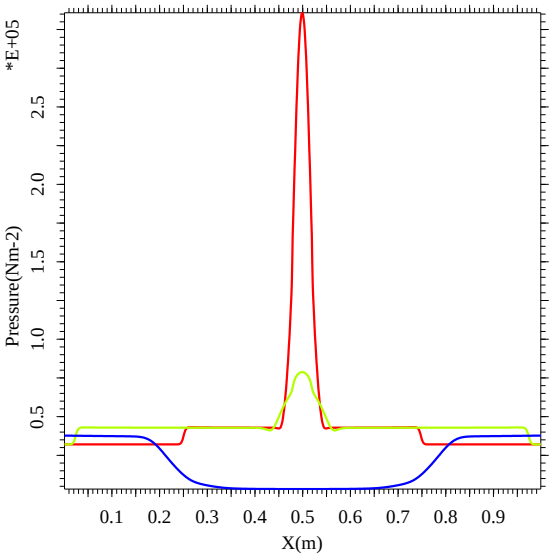

Figure 1.d. Pressure profile, at $0.5\mu s$(red), $1\mu s$ (green) and at $5\mu s$ (blue).

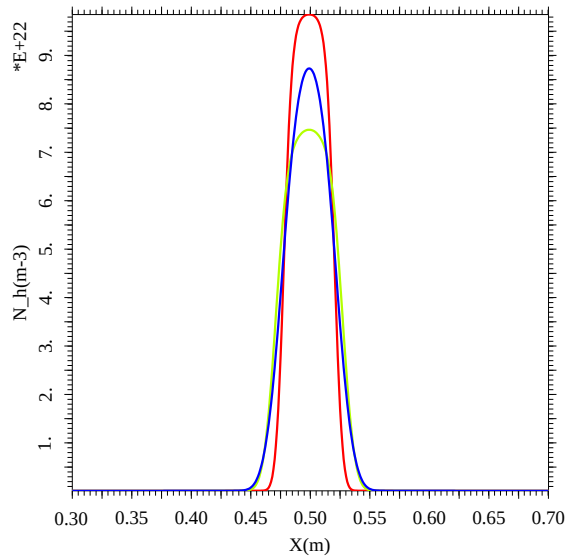

Figure 2.a. Particle density profile, at 1.0μs(red), 2.5μs (green) and at 5μs (blue).

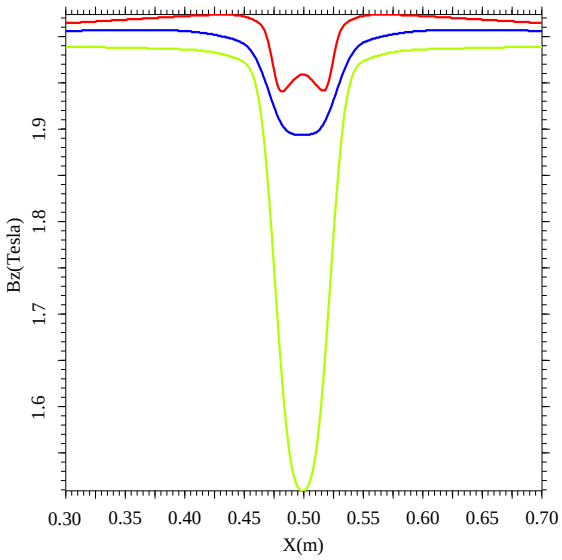

Figure 2.b. Magnetic field profile, at 1.0μs(red), 2.5μs (green) and at 5μs (blue).

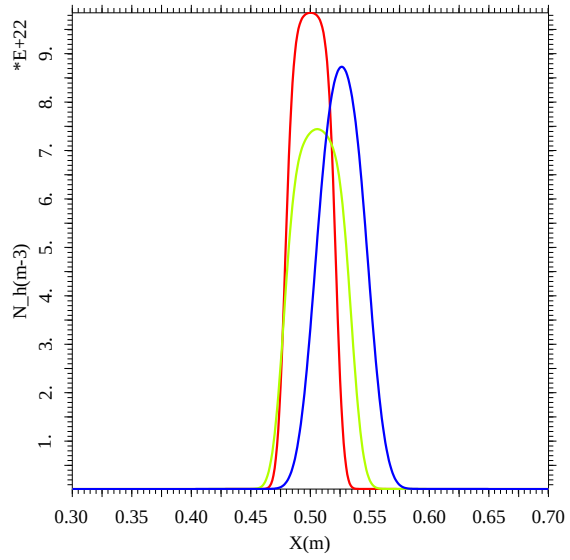

Figure 3.a. Particle density profile, at 1.0μs(red), 2.5μs (green) and at 5μs (blue).

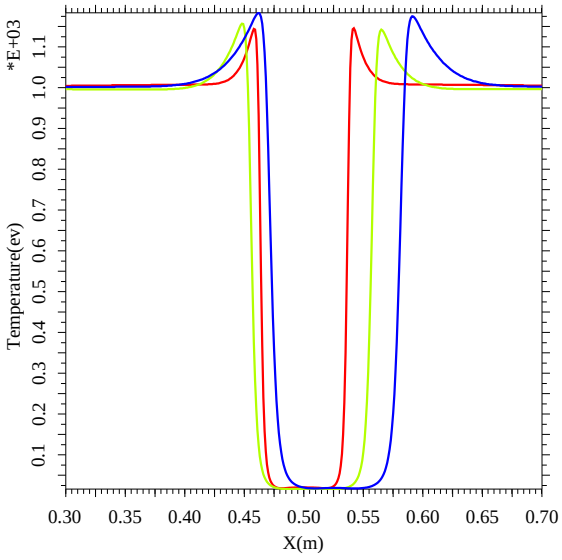

Figure 3.b. Temperature profile, at 1.0μs(red), 2.5μs (green) and at 5μs (blue).